

METAL-METAL CHARGE TRANSFER IN L_nM -CN- $FeCl_3$ COMPLEXES

Sheng, T.; Vahrenkamp, H.*

Institut für Anorganische und Analytische Chemie der Universität Freiburg,
Albertstr. 21, D-79104 Freiburg, Germany

Fax: +49-761-203-6001, E-mail: vahrenka@uni-freiburg.de

* Corresponding author

*Received November 10th, 2004. In final form November 27th, 2004
Dedicated to Professor Pedro Aymonino on the occasion of his 75th birthday*

Abstract

By combining the organometallic cyanides L_nM -CN [$L_nM = Cp(dppe)Fe$, $Cp(dppe)Ru$, $Cp(PPh_3)_2Ru$] with $FeCl_3$ the dinuclear complexes L_nM -CN- $FeCl_3$ were obtained. Structure determinations have revealed configurations close to linear arrays $Fe-C-N-Fe$ and $Ru-C-N-Fe$. From the $n(CN)$ band positions in their IR spectra it can be concluded that $FeCl_3$ is a very strong electron acceptor. Accordingly, the redox potentials of the L_nM -CN units are raised significantly upon attachment of $FeCl_3$. In the visible range of the electronic spectra the complexes show a strong metal-metal charge transfer band, the energy of which is a measure of the electron donating strength of the L_nM units. An analysis of the MMCT bands and their solvent dependency resulted in quantitative data on the metal-metal interactions.

Resumen

Al combinar los cianuros organometálicos L_nM -CN [$L_nM = Cp(dppe)Fe$, $Cp(dppe)Ru$, $Cp(PPh_3)_2Ru$] con $FeCl_3$ se obtuvieron los complejos dinucleares L_nM -CN- $FeCl_3$. Determinaciones estructurales han revelado formaciones $Fe-C-N-Fe$ y $Ru-C-N-Fe$ casi lineales. A partir de la posición de la banda $n(CN)$ en los espectros IR puede deducirse que el $FeCl_3$ es un aceptor de electrones muy fuerte. De acuerdo con esto, los potenciales rédox de las unidades L_nM -CN aumentan significativamente debido a la unión con $FeCl_3$. En la región visible de los espectros electrónicos los complejos muestran una banda intensa de transferencia de carga metal-metal, cuya energía es una medida de la fuerza de donación electrónica de las unidades L_nM . Un análisis de las bandas MMCT y su dependencia del disolvente dió como resultado datos cuantitativos sobre las interacciones metal-metal.

Introduction

Coordination polymers with cyanide-linked metal centers have attractive spectroscopic, magnetic and electrical properties[1,2]. The basis for these are metal-metal interactions across the bridging cyanide ligands. In low-molecular cyanide-bridged complexes these interactions express themselves in the redox properties as well as the vibrational and electronic spectra of the compounds[3]. Accordingly the study of di- and trinuclear cyanide-bridged complexes has yielded essential informations on the electronic communication between metal centers across bridging cyanide ligands.

In our recent review we have outlined the value of such studies and listed the contributions of the competing research groups in the field. Our own contributions are mainly concerned with linear arrays of the type $M'-CN-M-CN-M'$ with building blocks containing the metals M and M' in high and low oxidation states[4-8]. However, we also studied a series of dinuclear complexes of the type $M-CN-M'$ in which one of the two interconnected centers is an organometallic complex[9-13].

The present paper describes part of our attempts to simplify the $M-CN-M'$ systems even further by using the simplest building blocks in the form of the metal halides. A few studies of this kind have already been reported by Connelly and ourselves, for instance by attaching L_nM-CN units to $MnCl_2$, $CoCl_2$ and $NiCl_2$ [14], to $ZnCl_2$ [15], to $ZnBr_2$ and CdI_2 [16], and to $CuCl$ and $CuCl_2$ [12]. We now used $FeCl_3$ for this purpose which, due to the higher oxidation state of iron, should attract a stronger flow of electron density across the cyanide bridge. The results obtained by attaching organometallic cyanides to $FeCl_3$ have verified this expectation.

Experimental Section

The general working and measuring procedures were as described in Ref.[9]. The organometallic cyanides $Cp(dppe)Fe-CN$, $Cp(dppe)Ru-CN$ and $Cp(PPh_3)_2Ru-CN$ were prepared according to published procedures[17]. $FeCl_3$ was applied in the form of $FeCl_3 \cdot 2Py$ which was prepared as follows:

$FeCl_3$ (278 mg, 1.72 mmol) was added to 8 ml of pyridine and stirred for 2 h resulting in a red solution. 15 ml of diethyl ether and 10 ml of petroleum ether (60-70°C) were added and the resulting slurry was filtered. The filtrate was kept in a refrigerator to precipitate 450 mg (82%) of $FeCl_3 \cdot 2Py$ as yellow microcrystals, m.p. 74°C, which were filtered off, washed with diethyl ether and dried in vacuo.

$C_{10}H_{10}FeCl_3N_2$ (310.41) calcd.: C 37.49, H 3.15, N 8.74; found: C 37.13, H 3.29, N 8.67.

Complexes: 1: $Cp(dppe)Fe-CN$ (226 mg, 0.41 mmol) was added to a solution of $FeCl_3 \cdot 2Py$ (122 mg, 0.38 mmol) in 10 ml of ethanol. After refluxing for 5 h, cooling to room temp. and evaporation to 3 ml the product was chromatographed on a 1.5 x 10 cm silica gel column using acetone/dichloromethane (1/4) as eluent. A single blue band was collected. After evaporation of the eluate to dryness the residue was extracted with 8 ml of acetone. The extract was filtered and 1 ml of ethanol was added to the filtrate. Slow diffusion of diethyl ether into the solution yielded 138 mg (51%) of **1** as black crystals, m.p. 230°C (dec.).

$C_{32}H_{29}Cl_3Fe_2NP_2$ (707.59) calcd.: C 54.32, H 4.13, N 1.98; found: C 54.35, H 3.83, N 1.92.

2: $Cp(dppe)Ru-CN$ (134 mg, 0.23 mmol) was added to a solution of $FeCl_3 \cdot 2Py$ (64 mg, 0.20 mmol) in 15 ml of methanol. After stirring for 7 h and evaporation to dryness the residue was extracted with 2 ml of acetone and 1 ml of methanol. After filtration, slow diffusion of diethyl ether into the solution yielded 120 mg (80%) of **2** as black crystals, m.p. 240°C (dec.).

$C_{32}H_{29}Cl_3FeNP_2Ru$ (752.06) calcd.: C 51.06, H 3.88, N 1.86; found: C 51.17, H 3.71, N 1.70.

3: A solution of $Cp(PPh_3)_2Ru-CN$ (72 mg, 0.10 mmol) in 5 ml of dichloromethane was added to a solution of $FeCl_3 \cdot 2Py$ (32 mg, 0.10 mmol) in 5 ml of methanol and the mixture stirred for 4 h. After filtration, slow diffusion of diethyl ether into the solution yielded 52 mg (57%) of **3** as black crystals, m.p. 240°C (dec.).

$C_{42}H_{35}Cl_3FeNP_2Ru \cdot 0.5CH_3OH$ (878.92 + 16.02) calcd.: C 56.98, H 4.17, N 1.57; found: C 55.99, H 4.33, N 1.41.

Structure Determinations: Crystals of **1-3** were obtained by slow diffusion of diethyl ether into solutions of **1-3** in acetone. Diffraction data were recorded at -60°C on a Bruker Smart CCD diffractometer and subjected to empirical absorption corrections. The structures were solved and refined with the SHELX program suite [18]. All hydrogen atoms were included with fixed distances and isotropic temperature factors 1.2 times those of their attached atoms. Parameters were refined against F^2 . The R values are defined as $R_1 = \Sigma|F_o - F_c|/\Sigma F_o$ and $wR_2 = [\Sigma[w(F_o^2 - F_c^2)^2]/\Sigma[w(F_o^2)^2]]^{1/2}$. Drawings were produced with SCHAKAL [19]. Table 1 lists the crystallographic data.

CCDC-222555 (**1**), 222556 (**2**) and 222557 (**3**) contain the supplementary crystallographic data for this paper. These data can be obtained free of charge at www.ccdc.cam.ac.uk/conts/retrieving.html [or from the Cambridge Crystallographic Data Centre, 12, Union Road, Cambridge CB2 1EZ, UK; Fax: +44-1223/336-033; E-mail: deposit@ccdc.cam.ac.uk].

Table 1 Crystallographic details

	1	2	3
Empirical formula	$C_{32}H_{29}Cl_3Fe_2NP_2$	$C_{32}H_{29}Cl_3FeNP_2Ru$	$C_{42}H_{35}Cl_3FeNP_2Ru \cdot 0.5CH_3OH$
Molecular mass	707.55	752.77	894.94
Crystal size [mm]	035 x 0.1 x 0.1	0.65 x 0.2 x 0.15	0.4 x 0.25 x 0.1
Space group	Cc	Cc	$P2_1/n$
Z	4	4	4
a[Å]	10.625(1)	10.669(3)	10.472(2)
b[Å]	16.713(2)	17.054(5)	22.160(4)
c[Å]	18.023(2)	18.260(5)	17.514(3)
α [°]	90	90	90
β [°]	103.434(2)	104.046(5)	97.481(4)
γ [°]	90	90	90
V[Å ³]	3112.9(5)	3223.1(16)	4029.8(13)
d(calc)[gcm ⁻³]	1.51	1.55	1.48
μ (Mo-K α) [mm ⁻¹]	1.32	1.29	1.05
hkl range	h: -14 to 14 k: -22 to 21 l: -23 to 23	h: -14 to 14 k: -23 to 22 l: -24 to 16	h: -14 to 14 k: -29 to 29 l: -23 to 23
Measured reflections	13893	10490	36861

Table 1 continuing

Independent reflections	7147	5879	10028
Observed refl. [$I > 2\sigma(I)$]	5259	4289	6128
Parameters	361	361	466
Refined reflections	7147	5879	10028
R_1 (obs.refl.)	0.042	0.037	0.046
wR_2 (all refl.)	0.117	0.099	0.161
Residual electron density [$e/\text{\AA}^3$]	+0.7/-0.4	+0.7/-0.6	+1.4/-0.8

Results and Discussion

Preparations and Structures: As a starting material for FeCl_3 we chose its pyridine adduct of composition $\text{FeCl}_3 \cdot 2\text{Py}$ which has a good solubility in common organic solvents. Its combination with the organometallic cyanides in methanol or ethanol produced good yields of the dinuclear complexes **1-3**. The complexes are deeply coloured (blue to purple) in solution and form black crystals.

$\text{Cp}(\text{dppe})\text{Fe}-\text{CN}-\text{FeCl}_3$

1

$\text{Cp}(\text{dppe})\text{Ru}-\text{CN}-\text{FeCl}_3$

2

$\text{Cp}(\text{PPh}_3)_2\text{Ru}-\text{CN}-\text{FeCl}_3$

3

All three complexes were identified by crystal structure determinations (for details see Experimental Section). **1** and **2** are isostructural, and the atomic disposition in **3** is very similar. Hence only one structural drawing will be presented here: Figure 1 displays the structure of **1**. Bond lengths and angles are listed for comparative purposes in Table 2.

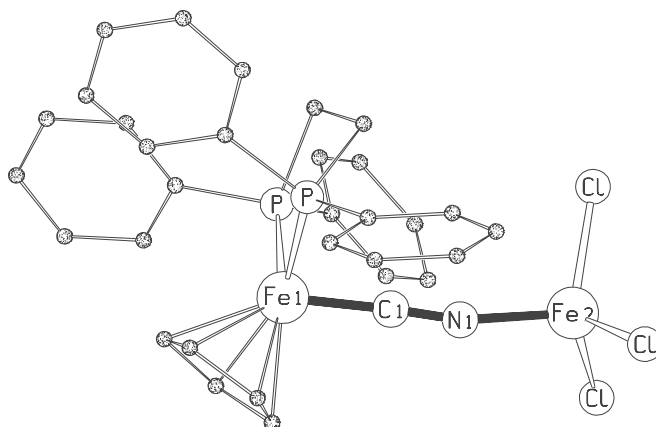


Figure 1. Molecular structure of complex **1**

The structures of complexes **1-3** are essentially superpositions of the structures of their two constituents, L_nM-CN and $L\bullet FeCl_3$. We have described many structures of oligonuclear complexes containing $Cp(dppe)Fe$ and $Cp(PPh_3)_2Ru$ units[4-13], and there are several $L\bullet FeCl_3$ structures in the literature[20,21]. Compared to the literature data,

Table 2. Relevant bond lengths (\AA) and angles ($^\circ$) in Complexes **1-3**

	1	2	3
Fe(Ru)-C1	1.808(5)	1.927(6)	1.935(4)
Fe-N1	1.904(4)	1.902(5)	1.918(4)
C1-N1	1.17(1)	1.17(1)	1.16(1)
Fe(Ru)-P(av.)	2.201(2)	2.291(1)	2.314(1)
Fe-Cl(av.)	2.190(2)	2.179(3)	2.171(3)
Fe(Ru)-C-N	175.2(4)	175.6(5)	174.8(4)
Fe-N-C	163.1(4)	164.7(5)	177.7(4)
N-Fe-Cl(av.)	107.5(2)	107.4(2)	108.0(2)
Cl-Fe-Cl(av.)	111.3(2)	111.5(2)	110.8(2)

both the Fe(Ru)-C1 bond and the Fe-N1 bond in **1-3** are relatively short. This finds its explanation in the IR data (see below) which also point to relatively weak C-N bonds. Yet the C-N bond lengths are notoriously insensitive to C-N bond strength changes, and therefore the C-N bond lengths observed for **1-3** are not unusually long.

The Fe and Ru atoms in the L_nM-CN units have the usual piano stool geometry with P-M-P and P-M-C angles near 90° . The N- $FeCl_3$ units are close to ideally tetrahedral, all valence angles being between 107.5 and 111.5 degrees. The angles along the M-C-N-Fe chains show their typical values[4-13]. While the M-C π -bonding (see below) forces the M-C-N angles to be close to 180° , there is no such constraint on the Fe-N-C angles. They vary much more and they can deviate significantly from 180° , as seen here for complexes **1** and **2**.

IR Spectroscopy and Electrochemistry: The characteristic feature in the IR spectra is the $\nu(CN)$ band (see Table 3), the position of which yields the essential bonding information.

Table 3. $\nu(CN)$ bands in the IR spectra of complexes **1-3** and their constituents (in KBr, cm^{-1}).

	$\bar{\nu}(CN)$	$\Delta \bar{\nu}$
$Cp(dppe)Fe-CN$	2062	
$Cp(dppe)Ru-CN$	2067	
$Cp(PPh_3)_2Ru-CN$	2072	
$Cp(dppe)Fe-CN-FeCl_3$ (1)	1986	-76
$Cp(dppe)Ru-CN-FeCl_3$ (2)	2003	-64
$Cp(PPh_3)_2Ru-CN-FeCl_3$ (3)	2013	-59

Normally one would expect that the kinematic effect, i.e. the impediment of the C-N vibration due to the attachment of the second metal atom, would increase $\nu(\text{CN})$ of the $L_n\text{M-CN}$ units upon attachment of the FeCl_3 groups. We have actually observed this raise of $\nu(\text{CN})$ in cases where the acceptor properties of the complex unit attached to the nitrogen of $\text{Cp}(\text{dppe})\text{Fe-CN}$ and $\text{Cp}(\text{PPh}_3)_2\text{Ru-CN}$ are low[9]. Yet as a rule the $\nu(\text{CN})$ values change little, and sometimes are even lowered in di- and trinuclear cyanide-bridged complexes[4-13]. The reason for this is a transfer of electron density along the M-C-N-M' chain. If M' is a strong electron acceptor, it will withdraw electron density through the N-M' σ -bond. This in turn induces enhanced π -backdonation from M into the cyanide's π -system. This populates the π^* orbitals, thereby weakening the C-N bond. In the case of complexes **1-3** this effect is stronger than ever observed before, with a lowering of $\nu(\text{CN})$ by $60\text{-}80\text{ cm}^{-1}$. As seen above from the structure determinations, this does not result in a significant lengthening of the C-N bonds. But the concomitant strengthening of both the M-C and N-Fe bonds is evident, supporting the interpretation of the IR data.

The cyclic voltammograms of complexes **1-3** show two reversible redox waves, cf. Table 4. As can be seen by comparison, the waves at higher potentials belong to the $L_n\text{M-CN}$ units. They are unusually high, compared to other dinuclear complexes derived from these $L_n\text{M-CN}$ units[4,9]. While it is to be expected that attachment of a Lewis acid at the CN's nitrogen withdraws electron density from $L_n\text{M}$, the FeCl_3 unit as a Lewis acid exerts this property in a hitherto unobserved extent. The cyclovoltammetric data are thus in full accord with the large band shifts of the $\nu(\text{CN})$ absorptions.

Table 4. Cyclovoltammetric data of complexes **1-3** and their constituents (in CH_2Cl_2 , potentials in V vs Ag/AgCl , scan rate 100 mV/s)

Complex	$E_{1/2}(1)\text{FeCl}_3$	$E_{1/2}(2)L_n\text{M}$	ΔE
$\text{Cp}(\text{dppe})\text{Fe-CN}$		0.48	
$\text{Cp}(\text{dppe})\text{Ru-CN}$		0.81	
$\text{Cp}(\text{PPh}_3)_2\text{Ru-CN}$		0.79	
1	-0.14	0.91	1.05
2	-0.06	1.40	1.46
3	-0.14	1.13	1.27

In accord with this the potentials for the FeCl_3 units in Table 4 show that the FeCl_3 units are rather easy to reduce, due to attachment of the rather electron-rich nitrogen donors $L_n\text{M-CN}$. Thereby the shift of electron density across the cyanide bridges has raised the redox potentials of both constituents of the dinuclear complexes by about the same amount. The potential differences of 1.05-1.46 V translate into an energy difference of about 10000 cm^{-1} (see below) which indicates that a metal metal charge transfer should be observable in the visible or NIR range of the electronic spectra, as was borne out by observation.

Metal-Metal Charge Transfer: The absorptions in the electronic spectra of complexes **1-3** and their constituents are listed in Table 5. Figure 2 shows the spectra for **2** as a representative example. Up to 400 nm the UV-Vis spectrum of **2** is a superposition of the spectra of $\text{Cp}(\text{dppe})\text{Ru}$ -

CN and $Py \cdot FeCl_3$. But the dominating feature in the visible range is the broad metal-metal charge transfer (MMCT) band. The occurrence of this band puts complexes **1-3** into class II of the mixed-valent species according to the classification of Robin and Day[22]. From the oxidation states of the metals and the redox potentials in Table 3 it is clear that the direction of the MMCT is $L_nM \rightarrow FeCl_3$. The asymmetry of the MMCT bands for **1** and **2** points to a spin-orbit splitting effect, due to the asymmetrical low-spin d^5 ions in $Cp(dppe)Fe$ and $Cp(dppe)Ru$ [23].

Table 5. Electronic spectra in dichloromethane solution

Complex	$\lambda_{max} (\epsilon_{max})$ [nm($\times 10^{-3} M^{-1} \cdot cm^{-1}$)]
$Cp(dppe)FeCN$	250 (8.54), 302 (2.28)
$Cp(dppe)RuCN$	242 (8.79), 298 (3.24)
$Cp(PPh_3)_2RuCN$	246 (10.21)
$Fe(py)Cl_3$	250 (5.67), 314 (4.05), 362 (4.27)
$Cp(dppe)FeCNFeCl_3$ (1)	250 (18.42), 338 (10.03), 648 (6.06)
$Cp(dppe)RuCNFeCl_3$ (2)	248 (17.06), 334 (6.52), 494 (4.07)
$Cp(PPh_3)_2RuCNFeCl_3$ (3)	248 (20.09), 320(7.89), 528 (4.72)

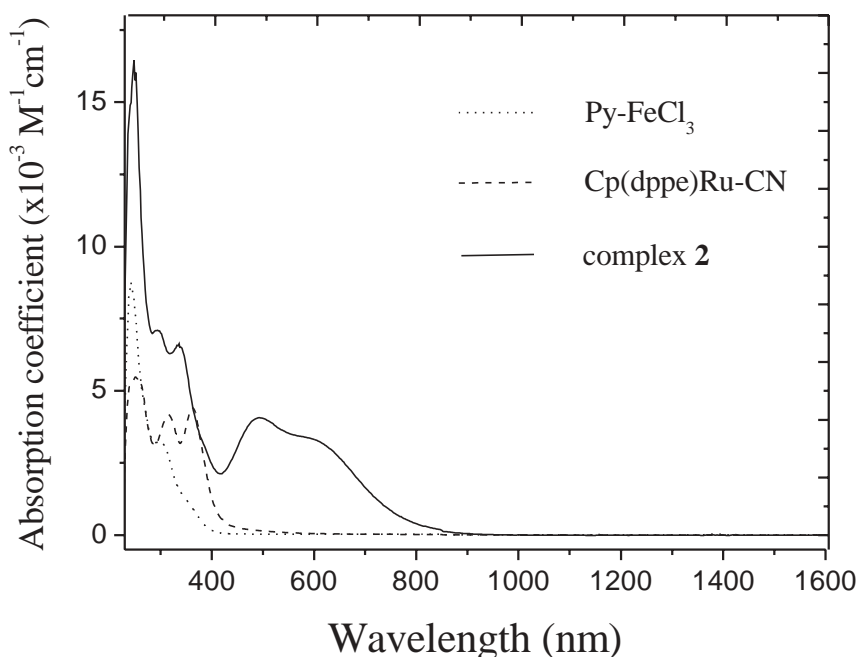


Figure 2. Electronic absorption spectra of complex **2** and its constituents in dichloromethane.

The analysis of the MMCT spectra can be performed according to equations (1) – (5), as developed by Hush for class II mixed-valent specie[24].

$$\Delta v_{1/2} = [2310 (v_{\max} - \Delta E_0)]^{1/2} \quad (1)$$

$$H_{\text{ab}} = v_{\max} \alpha = 2.06 \times 10^{-2} (v_{\max} / d) (\epsilon_{\max} \Delta v_{1/2} / v_{\max})^{1/2} \quad (2)$$

$$\alpha^2 = 4.24 \times 10^{-4} (\epsilon_{\max} \Delta v_{1/2} / v_{\max} d^2) \quad (3)$$

$$\Delta G^* = E_{\text{op}}^2 / 4\lambda_{\text{FC}} \quad (4)$$

$$E_{\text{op}} = \Delta E_0 + \lambda_{\text{FC}} \quad (5)$$

In the formulas $\Delta v_{1/2}$ is the bandwidth at half-intensity of the MMCT band with the maximum at v_{\max} ΔE_0 is the energy difference between the initial and final states of the electron transfer, ϵ_{\max} is the molar absorption coefficient at the MMCT band maximum. The metal-metal interaction and the electron delocalization parameters are H_{ab} and α^2 respectively, and d is the through space intermetallic distance. ΔG^* and λ_{FC} are the activation barrier for thermal electron transfer and the Franck-Condon barrier to electron transfer (reorganization energy), respectively. E_{op} is the measured energy of the MMCT band.

Applying the formulas the data in Table 6 can be computed. For this purpose ΔE_0 was approximated as the difference between the redox potentials $E_{1/2}$ (1) and $E_{1/2}$ (2) in Table 3, and the intermetallic distances of 4.8 Å in **1**, 4.9 Å in **2** and 5.0 Å in **3** were used in the calculations.

Table 6. Observed and calculated MMCT properties for **1-3** in dichloromethane^a

Complex	E_{op} (cm^{-1})	ϵ_{\max} ($M^{-1}\text{cm}^{-1}$)	$\Delta E_{1/2}$ (V) ^b	ΔE_0 (cm^{-1}) ^c	$(\Delta v_{1/2})_c$ (cm^{-1}) ^d	$(\Delta v_{1/2})_o$ (cm^{-1}) ^e
1	15432	6050	1.05	8476	4007	7513
2	20243	4070	1.46	11785	4420	7629
3	18939	4720	1.27	10251	4479	5442
	α^2 (%)	H_{ab} (cm^{-1})	ΔG^* (Kcal-mol ⁻¹)	$\bullet G'$ (Kcal-mol ⁻¹) ^e	λ_{FC} (cm^{-1})	
1	5.42	3592	24.42	0.24	6956	
2	2.71	3332	34.56	0.94	8458	
3	2.30	2872	29.45	0.20	8688	

^aThe following relations were used in this calculation: 1 eV = 8072 cm^{-1} , 1 Kcal-mol⁻¹ = 350.5 cm^{-1} .

^bDifference of oxidation potentials between initial and final states of the MMCT. ^cConverted from $\Delta E_{1/2}$.

^dCalculated half-width of the MMCT band with $(\Delta v_{1/2})_c = [2310 (E_{\text{op}} - \Delta E_0)]^{1/2}$ ^e Observed half-width of the MMCT band. ^eActivation barrier for the reverse thermal electron transfer with $\Delta G' = \Delta G^* - \Delta E_0$.

It is obvious from the data in Table 6 that complexes **1-3** are Class II mixed valent compounds. As is to be expected[25] the calculated half-widths of the MMCT bands are smaller (about 20-40%) than the observed ones, which is consistent with previous observations[5]. The values of their α^2 range from 0.0230 to 0.0542, in agreement with those of related mixed valent cyanide-bridged di- and trinuclear complexes reported by us[4,5,9].

The reorganization energies are similar to those of mixed valent complexes previously reported[5,9], but smaller than those found in the complexes trans-[Cp(dppe)Fe(III)NCpPt(II)(py)₂CNFe(III)(dppe)Cp]⁴⁺, trans-[Cp(dppe)Fe(III)NCpPt(II)(CN)₂CNFe(III)(dppe)Cp]²⁺ and trans-

[Cp(dppe)Fe(III)NCPt(CN)₂CN-Ru(II)(PPh₃)₂Cp]⁺[4]. The reorganization energy (8426cm⁻¹, 24.2 kcal/mol) of the asymmetrical mixed valent cyanide-bridged dinuclear iron-complex 1 is somewhat greater than that of the symmetrical species [(CN)₅Fe(II)(μ-CN)Fe(III)(CN)₅]⁶⁻ (22 kcal/mol)[26]. The calculated activation barriers for the thermal electron transfer for Fe_A(II)→Fe_B(III) in 1 and Ru(II)→Fe(III) in 2 and 3 are all very large compared to the activation barriers for the reverse thermal electron transfer for Fe_A(III)←Fe_B(II) and Ru(III)←Fe(II).

The solvent dependency of the MMCT bands for 1-3 was also investigated. Because complexes 1-3 are difficult to dissolve in inorganic solvents and many organic solvents such as methanol and benzene, and because the MMCT bands disappeared in some organic solvents with bigger Gutmann's donor number such as N, N-dimethylformamide and dimethyl sulphoxide, the solvent dependency of the MMCT bands for 1-3 was investigated in only a few organic solvents. The data obtained in these solvents are listed in Table 7.

Table 7. MMCT data for complexes 1-3 in selected solvents.

Solvent	DN ^a	1/D _{op} - 1/D _s ^b	Basicity ^c	λ _{max} (nm)(ε/M ⁻¹ cm ⁻¹)		
				1	2	3
CH ₂ Cl ₂	1.0	0.380	0.80	648 (6050)	494 (4070)	528 (4720)
CH ₃ NO ₂	2.7	0.498	0.92	696 (3050)	526 (3170)	554 (3630)
CH ₃ CN	14.1	0.526	0.86	692 (4790)	520 (3550)	542 (3390)
CH ₃ COCH ₃	17	0.494	0.81	660 (3570)	500 (3040)	526 (3340)
CHCl ₃	4.0	-	0.73	626 (3946)	480 (3500)	514 (4330)
DMF	26.6	0.463	0.97	None	None	None

^aref. 27. ^bref. 28 ^cref. 29

It appears that there is no correlation between the MMCT energy E_{op} and (1/D_{op}-1/D_s)[28] for the solvents investigated, and the relationship between E_{op} and Gutmann's donor number (DN)[27] is not clearly observed. But there is a good correlation between E_{op} and the solvent's basicity[29]. Here "basicity" means the cation-solvating tendency, which is one of the parameters to express solvent properties[29]. The relationship between E_{op} and the solvent's basicity for complex 2 is shown in Fig. 3.

ΔE_{op} is the energy difference of the initial and final states in the MMCT. The larger the basicity of the solvent, the more stable the Cp(dppe)Fe(III)-unit in the final state is expected to be, whereas the influence of the solvent on the Cl₃Fe(III)-unit should be relatively small, because the coordination sphere of the Cl₃Fe(III)-unit is composed of three basic chloride atoms. Therefore, as the solvent's basicity increases, the ΔE₀ required for metal-metal charge transfer decreases, and E_{op} shifts to lower energies.

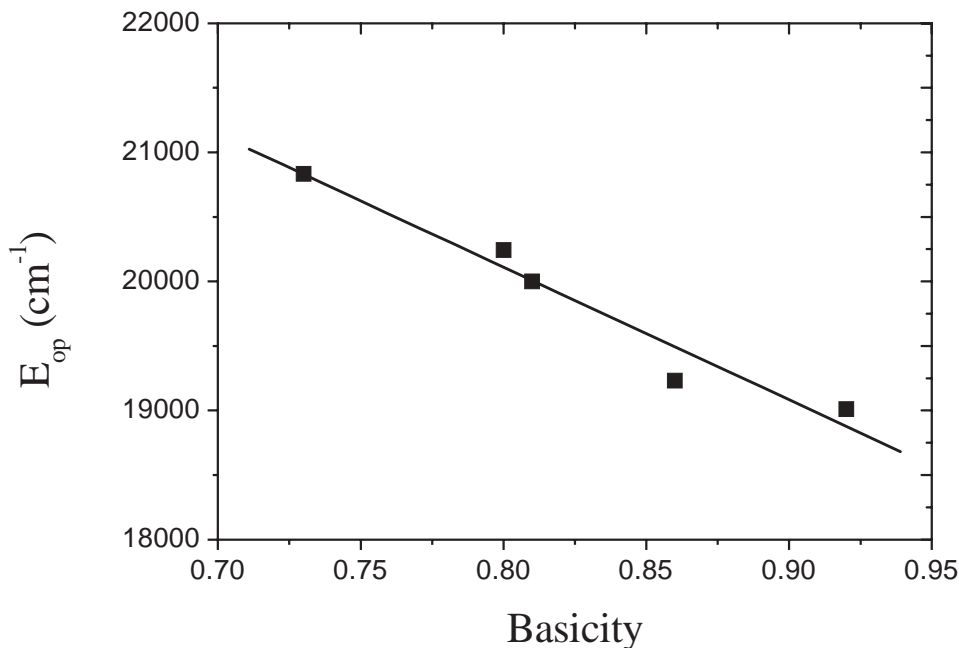


Figure 3. Relationship of the MMCT energy and the solvent's basicity[29] for complex 2

Conclusions

The combination of the organometallic cyanides and FeCl_3 was found to be facile, producing stable cyanide-linked dinuclear complexes with an inorganic oxidant at the nitrogen and an organometallic reductant at the carbon of the cyanide. An unusually strong shift of electron density from the organometallic units to FeCl_3 in these complexes is witnessed both by the $\nu(\text{CN})$ vibrations and the cyclovoltammetric redox waves. This shift results in a strengthening both of the M-C and the Fe-N bonds and a weakening of the C-N bonds. The linking via the cyanide bridges enables an optically induced metal-metal charge transfer, which corresponds to the redox transfer $\text{M(II)-CN-Fe(III)} \rightarrow \text{M(III)-CN-Fe(II)}$. An analysis of this metal-metal charge transfer using the Hush formalism has yielded metal-metal interaction parameters H_{ab} and delocalization parameters α^2 which are both large for this class of compounds. In summary it can be stated that the inorganic/organometallic combination offers high potential for the development of new cyanide-linked mixed-valent compounds.

Acknowledgement

This work was supported by the Deutsche Forschungsgemeinschaft (Graduiertenkolleg "Ungepaarte Elektronen") and by the Fonds der Chemischen Industrie.

References

- [1] Dunbar, K. R.; Heintz, R. A. *Prog. Inorg. Chem* **1997**, *45*, 283.
- [2] Bignozzi, C. A.; Schoonover, J. R.; Scandola, F. *Prog. Inorg. Chem.* **1997**, *44*, 1.
- [3] Vahrenkamp, H.; Geiß, A.; Richardson, G. N. *J. Chem. Soc. Dalton Trans.* **1997**, 3643.
- [4] Richardson, G. N.; Brand, U.; Vahrenkamp, H. *Inorg. Chem.* **1999**, *38*, 3070.
- [5] Geiß, A.; Kolm, M. J.; Janiak, G.; Vahrenkamp, H. *Inorg. Chem.* **2000**, *39*, 4037.

- [6] Chen, Z. N.; Appelt, R.; Vahrenkamp, H. *Inorg. Chim. Acta* **2000**, 309, 65.
- [7] Appelt, R.; Vahrenkamp, H. *Z. Anorg. Allg. Chem.* **2003**, 629, 133.
- [8] Flay, M.-L.; Vahrenkamp, H. *Eur. J. Inorg. Chem.* **2003**, 1719.
- [9] Zhu, N.; Vahrenkamp, H. *Chem. Ber.* **1997**, 130, 1241.
- [10] Geiß, A.; Vahrenkamp, H. *Eur. J. Inorg. Chem.* **1999**, 1793.
- [11] Comte, V.; Chen, Z. N.; Flay, M.-L.; Vahrenkamp, H. *J. Organomet. Chem.* **2000**, 614-615, 131.
- [12] Comte, V.; Vahrenkamp, H. *J. Organomet. Chem.* **2001**, 627, 153.
- [13] Appelt, R.; Vahrenkamp, H. *Inorg. Chim. Acta* **2003**, 350, 387.
- [14] Connelly, N. G.; Hicks, O. M.; Lewis, G. R.; Orpen, A. G.; Wood, A. J. *J. Chem. Soc. Dalton Trans.* **2000**, 1637.
- [15] Richardson, G. N.; Vahrenkamp, H. *J. Organomet. Chem.* **2000**, 593-594, 44.
- [16] Connelly, N. G.; Lewis, G. R.; Moreno, M. T.; Orpen, A. G. *J. Chem. Soc. Dalton Trans.* **1998**, 1905.
- [17] Baird, G. J.; Davis, S. G. *J. Organomet. Chem.* **1984**, 262, 215.
- [18] *SHELX* program package for the Bruker Smart CCD diffractometer, version 5.1, 2002
- [19] Keller, E.; *SCHAKAL for Windows*, Universität Freiburg, **2001**.
- [20] Wang, J.; Mashuta, M. S.; Sun, Z.; Richardson, J. F.; Hendrickson, D. N.; Buchanan, R. M. *Inorg. Chem.* **1996**, 35, 6642.
- [21] Steimann, M.; Nagel, U.; Grenz, R.; Beck, W. *J. Organomet. Chem.* **1983**, 247, 171.
- [22] Robin, M. B.; Day, P. *Adv. Inorg. Chem. Radiochem.* **1967**, 10, 247.
- [23] Kober, E. M.; Goldsby, K. A.; Narayana, D. N. S.; Meyer, T. J. *J. Am. Chem. Soc.* **1983**, 105, 4303.
- [24] Hush, N. S. *Prog. Inorg. Chem.* **1967**, 8, 391.
- [25] Creutz, C. *Prog. Inorg. Chem.* **1983**, 30, 1.
- [26] Glauser, R.; Hauser, U.; Herren, F.; Ludi, A.; Roder, P.; Schmidt, E.; Siegenthaler, H.; Wenk, F. *J. Am. Chem. Soc.* **1973**, 95, 6457.
- [27] Gutmann, V.; Wychera, E. *Inorg. Nucl. Chem. Lett.* **1966**, 2, 257.
- [28] Hupp, J. T.; Dong, Y.; Blackburn, R. L.; Lu, H. *J. Phys. Chem.* **1993**, 97, 3278.
- [29] Swain, C. G.; Swain, M. S.; Powell, A. L.; Alunni, S. *J. Am. Chem. Soc.* **1983**, 105, 502.